

GEOMETRIC STRUCTURE, ELECTRONIC STRUCTURE, AND SPIN TRANSITION OF Fe^{2+} SPIN-CROSSOVER MOLECULES

NGUYEN VAN THANH, NGUYEN THI NGUYET ANH, NGUYEN ANH TUAN
Faculty of Physics, Hanoi University of Science, Vietnam National University

Abstract. *We present a density functional study on the geometric structure, electronic structure and spin transition of a series of Fe^{2+} spin-crossover molecules, i.e., $[\text{Fe}(\text{abpt})_2(\text{NCS})_2]$ (1), $[\text{Fe}(\text{abpt})_2(\text{NCSe})_2]$ (2), and $[\text{Fe}(\text{abpt})_2(\text{C}(\text{CN})_3)_2]$ (3) with $\text{abpt} = 4\text{-amino-3,5-bis(pyridin-2-yl)-1,2,4-triazole}$ in order to shed light on more about the dynamics of the spin-crossover phenomenon. All results presented in this study were obtained by using the exchange correlation PBE functional. For better accuracy, the hexadecapolar expansion scheme is adopted for resolving the charge density and Coulombic potential. Our calculated results demonstrate that the transition between the low-spin (LS) and high-spin (HS) states of these Fe^{2+} molecules is accompanied with redistribution of atomic charge and reformation of molecular orbitals. These cause differences in the kinetic energy, the electrostatic energy as well as the total energy between the LS and HS states. The LS state is advantage in the kinetic energy in comparison to the HS state, while the HS state is advantage in the electrostatic energy. Moreover, the coulomb attraction energy between the Fe^{2+} ion and its surrounding anionic ions plays a crucial role for spin crossover occurring.*

I. INTRODUCTION

Transition metal complexes that exhibit a temperature dependent crossover from a low-spin (LS) state to a high-spin (HS) state have been prepared as early as 1908 [1]. In the last few decades, research into the preparation and properties of complexes that exhibit this effect has been extensive after it was discovered that spin state can be switched reversibly by pressure or light irradiation in solid samples [2] as well as in solutions [3]. Spin crossover (SCO) complexes are now very potential candidates for applications such as molecular switches, display and memory devices [4].

Although the phenomenon of SCO is theoretically possible for octahedral d^4 – d^7 ions, it is quite frequently observed in complexes containing Fe^{2+} and Fe^{3+} [5-7], and to a lesser extent in Co^{3+} as well as Mn^{2+} complexes. This situation highlights that to induce SCO in these complexes the ligands must impose a ligand field strength that results in a minimal difference between the octahedral splitting energy (Δ) and the electron spin pairing energy (P) in order for a minor perturbation results in switching between the LS and HS states. The electron spin pairing energy P strongly depends on nuclear charge of transition metal atoms. Indeed, a comparison between the Fe^{2+} and Co^{3+} complexes shows that, even though the Fe^{2+} and Co^{3+} ions have the same number of $3d$ electron (d^6), however, the Fe^{2+} complexes usually exhibit SCO phenomenon, while the Co^{3+} complexes with higher nuclear charge of Co^{3+} usually stabilizes the LS state with $S = 0$. Similarly, SCO is rarely observed in Mn^{2+} (d^5) complexes, in which the HS state is usually stabilized, in contrast to the isoelectronic Fe^{3+} ion, for which many examples of spin conversion exist [8].

As discussed above, the SCO phenomenon can be qualitatively explained by the ligand field model, however, this simple model is not enough to understand dynamics of the LS-HS transition, as well as to determine the total energy difference between the LS and HS states and the LS-HS transition temperature.

In this paper, to shed light on more about the dynamics of the SCO phenomenon, the geometric structure, electronic structure and spin transition of three Fe^{2+} spin-crossover molecules with different ligand configurations have been studied based on Density-functional theory. They have the general chemical formula $[\text{Fe}(\text{abpt})_2\text{X}_2]$ with $\text{abpt} = 4\text{-amino-3,5-bis(pyridin-2-yl)-1,2,4-triazole}$, and $\text{X} = \text{NCS}, \text{NCSe}, \text{and } \text{C}(\text{CN})_3$. Our calculated results demonstrate that the transition from the LS state to the HS states of these Fe^{2+} molecules is accompanied with charge (electron) transfer from the Fe atom to its surrounding ligands, as well as reformation of molecular orbitals. These processes make changes in the kinetic energy and the electrostatic energy as well as the total electronic energy. Moreover, not only the pairing energy, but also the coulomb attraction energy between the Fe ion and its surrounding anionic ligand ions play a crucial role for SCO occurring.

II. COMPUTATIONAL METHODS

All calculations have been performed by using the DMol³ code [9] with the double numerical basis sets plus polarization functional. For the exchange correlation terms, the generalized gradient approximation (GGA) PBE functional was used [10]. The effective core potential Dolg-Wedig-Stoll-Preuss was used to describe the interaction between the core and valence electrons [11]. The overlapped electronic cloud between iron ion with ligands in the LS and HS states are much complex. It has a big fault by using octupolar expansion scheme to compute the energy difference between the LS and HS states that is the total electronic energy of the HS state underlying that of the LS state. For better accuracy, the hexadecapolar expansion scheme was adopted for resolving the charge density and Coulombic potential. The atomic charge and magnetic moment were obtained by using the Mulliken population analysis [12]. The real-space global cutoff radius was set to be 4.6 Å for all atoms. The spin-unrestricted DFT was used to obtain all results presented in this study. The charge density is converged to 1×10^{-6} a.u. in the self-consistent calculation. In the optimization process, the energy, energy gradient, and atomic displacement are converged to 1×10^{-5} , 1×10^{-4} and 1×10^{-3} a.u., respectively. From the experimental crystal structure, the isolate single molecule has taken out then set in vacuum. In order to determine the ground-state atomic structure of the Fe^{2+} molecules, we carried out total-energy calculations with full geometry optimization, allowing the relaxation of all atoms in this molecule. In addition, to obtain both the geometric structures corresponding to the LS and HS states of the Fe^{2+} molecule, both the LS and HS configurations of the Fe^{2+} ion are probed, which are imposed as an initial condition of the structural optimization procedure. In terms of the octahedral field, the Fe^{2+} ion could, in principle, has the LS state with configuration $d^6(t_{2g}^6, e_g)$ and the HS state with configuration $d^6(t_{2g}^4, e_g^2)$. The spin transition states of these molecules were determined by using the Linear-Synchronous-Transit method [13].

III. RESULTS AND DISCUSSION

Three $[\text{Fe}(\text{abpt})_2\text{X}_2]$ ($\text{X} = \text{various}$) molecules have the same $[\text{Fe}(\text{abpt})_2]$ skeleton but different in the X ligand with $\text{X} = \text{NCS}$, NCSe , and $\text{C}(\text{CN})_3$ for **(1)**, **(2)**, and **(3)**, respectively, in which two equivalent chelating abpt ligands stand in the equatorial plane and two equivalent terminal nitrile anions (X) complete the coordination sphere in trans position, as shown in Fig. 1. These molecules have been fully optimized by using the above computational method. Their computed molecular geometric structures are slightly different from experimental data reported in references [14,15], as tabulated in Table 1. Here, it is noted that, these calculations have been carried out for isolated complexes in vacuum. This approximation neglects interactions between neighbouring molecules. Calculations which do not regard these interactions can therefore be different from the experiment. Nevertheless, such calculations for isolated molecules in vacuum may reveal information about the molecular contribution to substituent-induced shifts of SCO characteristics. This information can hardly be gained experimentally since any experiment with a solid sample will only reflect the combined influence of intra- and intermolecular interactions. Also we succeeded in predicting the geometric structure of the LS state of molecules **(1)** and **(2)** which are not available from experimental data.

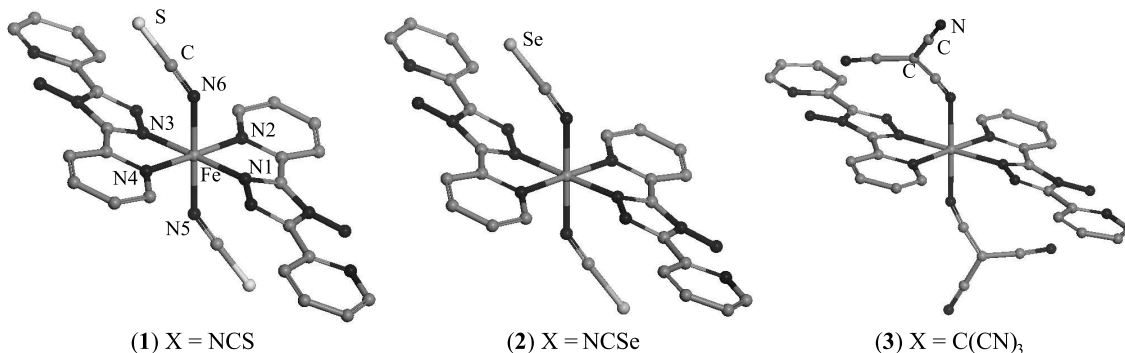


Fig. 1. Schematic geometric structure of molecules **(1)**, **(2)** and **(3)**. H atoms are removed for clarity.

As shown in Table 1, the Fe-N bond lengths of the LS state are always shorter than those of the HS state for all these Fe^{2+} molecules. This can be explained in terms of ligand field theory. In molecules **(1)**, **(2)**, and **(3)**, the Fe^{2+} ion is located in nearly octahedron forming by six anionic nitrogen ions, as shown in Fig. 1. In terms of octahedral ligand field, the LS state of the Fe^{2+} is (t_{2g}^6, e_g^0) characterized by three fully occupied t_{2g} orbitals ($d_{xy}^2, d_{xz}^2, d_{yz}^2$) and by two empty e_g orbitals ($d_{x^2-y^2}^0, d_{z^2}^0$). In the paramagnetic HS state with the electronic configuration (t_{2g}^4, e_g^2) , five electrons belonging to the majority spin are distributed over all five $3d$ orbitals according to Hund's rule, the sixth electron that belongs to the minority spin enters a t_{2g} orbital. It is easy to see that e_g orbitals are single occupied in the HS state, while they are empty in the LS state. As we know, the electron density in e_g orbitals is directed toward six anionic nitrogen ions surrounding the Fe^{2+} ion, while the electron density in t_{2g} orbitals is distributed along the bisector of the

Table 1. Fe-N bond lengths (in Å) and N-Fe-N bond angles (in degree) of the LS and HS states of **(1)**, **(2)** and **(3)** obtained from calculated results and experimental data [14,15]. Experimental values are shown in italic. The average values of Fe-N bond lengths and N-Fe-N bond angles are shown in bold.

	(1)			(2)			(3)			
	LS	HS		LS	HS		LS		HS	
Fe-N(1)	1.979	2.120	2.218	1.968	2.189	2.219	1.996	1.981	2.145	2.172
Fe-N(2)	1.986	2.205	2.212	1.991	2.105	2.205	2.022	2.008	2.187	2.195
Fe-N(3)	1.963	2.120	2.241	1.977	2.189	2.218	1.996	1.964	2.145	2.167
Fe-N(4)	1.992	2.205	2.208	1.990	2.105	2.205	2.022	2.001	2.187	2.194
Fe-N(5)	1.960	2.120	2.060	1.955	2.131	2.073	1.941	1.902	2.139	2.075
Fe-N(6)	1.958	2.120	2.062	1.955	2.131	2.073	1.941	1.915	2.139	2.102
	1.973	2.148	2.167	1.973	2.142	2.166	1.986	1.962	2.157	2.151
N(1)-Fe-N(2)	81.058	75.000	75.263	80.826	74.000	75.603	80.182	80.549	75.664	75.883
N(2)-Fe-N(3)	99.213	105.000	103.080	99.249	105.100	104.354	99.818	99.184	104.336	104.555
N(3)-Fe-N(4)	80.778	75.000	75.224	80.819	74.000	75.601	80.182	80.581	75.664	76.316
N(1)-Fe-N(5)	83.713	89.800	84.105	84.115	89.400	83.202	91.457	92.903	91.662	85.591
N(4)-Fe-N(5)	93.457	92.500	91.728	92.334	92.300	92.975	89.547	88.691	88.960	92.328
N(1)-Fe-N(6)	96.610	90.200	93.475	95.472	90.600	96.716	88.543	85.152	88.338	95.003
N(4)-Fe-N(6)	86.922	87.500	87.629	87.364	87.700	86.960	90.453	92.596	91.040	86.337
N(1)-Fe-N(4)	98.977	105.000	106.543	99.122	105.100	104.441	99.818	99.689	104.336	103.250
N(2)-Fe-N(5)	87.722	87.500	86.569	86.726	87.700	86.960	90.453	90.876	91.040	86.549
N(3)-Fe-N(5)	90.200	87.500	99.578	96.812	90.600	96.801	88.543	87.436	88.338	94.584
N(2)-Fe-N(6)	91.900	92.500	94.166	93.575	92.300	93.105	91.457	87.844	88.960	94.790
N(3)-Fe-N(6)	84.589	89.800	82.885	83.551	89.400	83.282	89.547	94.504	91.662	84.812
	89.595	89.775	90.020	89.997	89.850	90.000	90.000	90.000	90.000	90.000

N-Fe-N angles. Therefore, coulomb repulsion to anion nitrogen ions from e_g electrons is stronger than that from t_{2g} electrons. Consequently, the Fe-N bond lengths of the HS state are longer than those of the LS state. As shown in Table 1, the Fe-N bond lengths are typically about 1.95 to 2.02 Å in the LS state, increase by about 10% upon crossover to the HS state.

Previous experimental studies reported that the SCO temperature (T_{SCO}) of **(1)**, **(2)** and **(3)** is significantly different even though their mean values of Fe-N bond lengths are only slightly different. The T_{SCO} is 180, 224 and 336 K for **(1)**, **(2)** and **(3)**, respectively. These results demonstrate that the mean value of Fe-N bond lengths is not enough to determine the T_{SCO} of Fe^{2+} molecules. The T_{SCO} can be estimated by a simple model [16,17] that is restricted to isolated molecules and requires only the knowledge of the difference $\Delta F = F_{HS} - F_{LS}$ between the free energy of the HS and LS states. In this model the temperature dependence of the molar HS fraction γ_{HS} can be written as Eq. (1).

$$\gamma_{HS} = \frac{1}{\left[1 + \exp\left(\frac{\Delta F}{k_B T}\right)\right]} \quad (1)$$

The free energy difference is a sum of three terms, the electronic energy difference ΔE , the vibrational energy difference ΔE_{vib} , and the entropy difference multiplied by the temperature as Eq. (2).

$$\Delta F = \Delta E + \Delta E_{vib} - T\Delta S(T) \quad (2)$$

Only the latter two terms on the right side of Eq. (2) are temperature dependent, whereas the electronic energy difference, which is in the order of a few thousand Kelvin, is in good approximation temperature independent. With the help of Equations 1 and 2

the transition temperature T_{SCO} , that is implicitly defined by $\gamma_{HS}(T_{SCO}) = 1/2$, can be written as Eq. (3).

$$T_{SCO} = \frac{\Delta E + \Delta E_{vib}}{\Delta S(T_{SCO})} \quad (3)$$

Neglecting the vibrational energy difference ΔE_{vib} , which is rather small in comparison with the electronic energy difference ΔE and in the range of the error margin of ΔE [18], Eq. (3) simplifies to Eq. (4) where ΔS_{SCO} denotes entropy difference at the transition temperature.

$$T_{SCO} = \frac{\Delta E}{\Delta S_{SCO}} \quad (4)$$

From the two quantities on the right side of Eq. (4) it seems to be the electronic energy difference ΔE , which is most sensitive upon small variations of the SCO molecules, such as substitutions on the ligands. Considering a given class of similar SCO complexes, one may as a crude approximation take the entropy difference at the transition temperature as a constant proportionality factor and write simply Eq. (5).

$$T_{SCO} \sim \Delta E \quad (5)$$

From Eq. (5), it is expected that the higher T_{SCO} , the higher electronic energy difference between the HS and LS states (ΔE). Indeed, our calculated results show that molecules **(1)**, **(2)** and **(3)** have ΔE of 0.14, 0.18 and 0.20 eV, respectively. It poses a question what makes the difference in ΔE between these molecules. To shed light on this question, we carried out calculating energy components, including the kinetic energy (K), the electrostatic energy ($E_{coulomb}$) and the exchange-correlation energy (E_{xc}). The values of K , $E_{coulomb}$ and E_{xc} of the LS and HS states of **(1)**, **(2)** and **(3)** are tabulated in Table 2. The difference in K , $E_{coulomb}$ and E_{xc} between the LS and HS states of **(1)**, **(2)** and **(3)** is also listed in Table 2. As shown in Table 2, the kinetic energy difference and the electrostatic energy difference between the HS and LS states are significant in comparison to the total electronic difference for all these Fe^{2+} molecules, while the exchange-correlation energy difference between the HS and LS states is always small. These results demonstrate that the total electronic energy difference is mainly contributed by the kinetic energy difference and the electrostatic energy difference. The electrostatic energy difference between the HS and LS states is negative for all these Fe^{2+} molecules, and its absolute value increases in order of **(1)**, **(2)** and **(3)**. In contrast, the kinetic energy difference between the HS and LS states is positive for all these Fe^{2+} molecules, and increases in order of **(1)**, **(2)** and **(3)**. Therefore, the disadvantage in the kinetic energy of the HS state in comparison to the LS state is the reason for the total electronic energy of the HS state being higher than that of the LS state. Also, these results reveal correlations among the total electronic energy difference, the kinetic energy difference, the electrostatic energy difference and the SCO temperature of these Fe^{2+} molecules. One may say that the SCO temperature of these Fe^{2+} molecules is proportional to these energy differences.

As mentioned above, the kinetic energy of the LS state is more negative than that of the HS state for all these Fe^{2+} molecules. This can be understood in terms of molecular orbitals (MOs). In a molecule, MOs are formed by hybridization between atomic

Table 2. The calculated energy components of the LS and HS states of **(1)**, **(2)** and **(3)**, including the kinetic energy (K), the electrostatic energy ($E_{coulomb}$) and the exchange-correlation energy (E_{xc}).

Energy component (eV)	(1)			(2)			(3)		
	LS	HS	HS-LS	LS	HS	HS-LS	LS	HS	HS-LS
K	-380.53	-373.25	7.28	-447.50	-431.47	16.03	-636.34	-617.59	18.76
$E_{coulomb}$	-195.27	-202.39	-7.12	-125.45	-141.24	-15.79	-37.45	-56.07	-18.62
E_{xc}	140.57	140.55	-0.02	139.72	139.65	-0.07	163.60	163.67	0.07
Total			0.14			0.18			0.20

orbitals. Weak hybridization will leads MOs to mainly localize at each atom, and strong hybridization will leads to MOs expanding over whole molecule. The later is advantage in kinetic energy than the former. It is noted that Fe-N bond lengths of the LS state are smaller than those of the HS state. Therefore, hybridization among atomic orbitals in the LS state is stronger than that in the HS state. Consequently, the LS state is advantage in kinetic energy than the HS state.

Also, as presented above, the electrostatic energy of the HS state is more negative than that of the LS state, even though the Fe-N bond lengths of the LS state are smaller than those of the HS state. This is due to disadvantage in pairing energy of the LS state in comparison to the HS state. However, the electron-electron pairing energy is usually in the range of 2–3 eV. Therefore, only the disadvantage in pairing energy of the LS state in comparison to the HS state is not enough to explain magnitude of difference in the electrostatic energy between the LS and HS states of **(1)**, **(2)** and **(3)**. The electrostatic energy differences between the LS and HS states of **(1)**, **(2)** and **(3)** are several times larger than the pairing energy, as shown in Table 2. As we known, the transition from the LS state to the HS state is accompanied with expansion of bond lengths, especially the bonds between the Fe and six surrounding N atoms. This can cause redistribution of atomic charge, especially charge of the Fe and six surrounding N atoms. To elucidate this, the atomic charge of **(1)**, **(2)** and **(3)** has been calculated. Our calculated results show that the atomic charge of **(1)**, **(2)** and **(3)** in the HS state is larger than that in the LS state, especially charge of the Fe and six surrounding N atoms, as tabulated in Table 3. For example, the charge of Fe atom in the HS state of **(3)** is over twice larger than that in the LS state, and the charge of N atoms increases by about 1.14 to 1.41 times upon crossover from the LS to the HS state. One may say that charge (electron) is transferred from the Fe ion to six surrounding N ions upon crossover from the LS to the HS state. This causes the Fe ion becoming more positive and six anionic N ions becoming more negative. Hence, the coulomb attraction energy between the Fe ion and six surrounding N ions becomes more negative by transition from the LS state to the HS state which contributes to advantage in the electrostatic energy of the HS state in comparison to the LS state.

IV. CONCLUSIONS

The geometric structure, electronic structure and spin transition of a series of three Fe²⁺ spin-crossover molecules have been studied based on Density-functional theory in

Table 3. The charge of Fe and six surrounding N atoms in the LS and HS states of (1), (2) and (3).

	(1)			(2)			(3)		
	n_{LS} (e)	n_{HS} (e)	n_{HS}/n_{LS}	n_{LS} (e)	n_{HS} (e)	n_{HS}/n_{LS}	n_{LS} (e)	n_{HS} (e)	n_{HS}/n_{LS}
Fe	0.419	0.858	2.048	0.432	0.870	2.014	0.387	0.870	2.248
N1	-0.230	-0.299	1.300	-0.228	-0.305	1.338	-0.245	-0.317	1.294
N2	-0.376	-0.419	1.114	-0.378	-0.422	1.116	-0.392	-0.448	1.143
N3	-0.227	-0.301	1.326	-0.230	-0.305	1.326	-0.248	-0.321	1.294
N4	-0.377	-0.417	1.106	-0.377	-0.422	1.119	-0.391	-0.450	1.151
N5	-0.334	-0.419	1.254	-0.202	-0.289	1.431	-0.235	-0.317	1.349
N6	-0.340	-0.408	1.200	-0.197	-0.290	1.472	-0.232	-0.327	1.409

order to shed light on more about the dynamics of the spin-crossover phenomenon. Our calculated results show that the transition from the LS state to the HS states is accompanied with charge (electron) transfer from the Fe atom to ligands, as well as reformation of molecular orbitals. These processes make changes in the kinetic energy and the electrostatic energy as well as the total electronic energy. The LS state is advantage in the kinetic energy in comparison to the HS state, while the HS state is advantage in the electrostatic energy. Moreover, our calculated results demonstrate that not only the pairing energy, but also the coulomb attraction energy between the Fe ion and its surrounding anionic N ions play a crucial role for SCO occurring. The results should be helpful for developing new SCO molecules.

ACKNOWLEDGMENTS

We thank Vietnam National University (Hanoi) for funding this work within project QG-11-05. The computations presented in this study were performed at the Information Science Center of Japan Advanced Institute of Science and Technology, and the Center for Computational Science of the Faculty of Physics, Hanoi University of Science, Vietnam.

REFERENCES

- [1] M. Delépine, *Bull. Soc. Chim. Fr.* **3** (1908) 643.
- [2] S. Decurtins, P. Gülich, C.P. Köhler, H. Spiering, A. Hauser, *Chem. Phys. Lett.* **139** (1984) 1.
- [3] J. J. McGarvey, I. Lawthers, *J. Chem. Soc., Chem. Commun.* (1982) 906.
- [4] H. A. Goodwin, P. Gülich, *Top. Curr. Chem.* **233** (2004) 1.
- [5] Jonathan A. Kitchen, Sally Brooker, *Coordination Chemistry Reviews* **252** (2008) 2072–2092.
- [6] Birgit Weber, *Coordination Chemistry Reviews* **253** (2009) 2432–2449.
- [7] Ivan Salitros, N. T. Madhu, Roman Boca, Jan Pavlik, Mario Ruben, *Monatsh Chem* **140** (2009) 695–733.
- [8] P. J. van Konigsbruggen, Y. Maeda, H. Oshio, *Top. Curr. Chem.* **233** (2004) 259–324.
- [9] B. Delley, *J. Chem. Phys.* **92** (1990) 508.
- [10] J. P. Perdew, K. Burke, M. Ernzerhof, *Phys. Rev. Lett.* **77** (1996) 3865.
- [11] M. Dolg, U. Wedig, H. Stoll, H. Preuss, *J. Chem. Phys.* **86** (1987) 866; A. Bergner, M. Dolg, W. Kuechle, H. Stoll, H. Preuss, *Mol. Phys.* **80** (1993) 1431.
- [12] R. S. Mulliken, *J. Chem. Phys.* **23** (1955) 1833; R. S. Mulliken, *J. Chem. Phys.* **23** (1955) 1841.
- [13] T. A. Halgren, W. N. Lipscomb, *Chem. Phys. Lett.* **49** (1977) 225.
- [14] Nicolás Moliner *et.al.*, *Inorganica Chimica Acta* **291** (1999) 279–288.

- [15] Gaelle Dupouy *et.al.*, *Inorg. Chem.*, **47** (2008) 8921-8931.
- [16] P. Gütlich, H. Köppen, R. Link, H. G. Steinhäuser, *J. Chem. Phys.* **70** (1979) 3977.
- [17] H. Paulsen; J. A. Wolny, A. X. Trautwein, *Monatshefte für Chemie* **136** (2005) 1107–1118.
- [18] H. Paulsen, L. Duelund, A. Zimmermann, F. Averseng, M. Gerdan, H. Winkler, H. Toftlund, A. X. Trautwein, *Monatsh Chem.* **134** (2003) 295.

Received 30-09-2011.